Understanding the Fundamental Connection Between Electronic Correlation and Decoherence

Arnab Kar, Liping Chen, and Ignacio Franco*

Department of Chemistry and The Center for Coherence and Quantum Optics, University of Rochester, Rochester, New York 14627, USA

Abstract

We introduce a theory that exposes the fundamental and previously overlooked connection between the correlation among electrons and the degree of quantum coherence of electronic states in matter. For arbitrary states, the effects only decouple when the electronic dynamics induced by the nuclear bath is pure-dephasing in nature such that $[H^S, H^{SB}] = 0$, where H^S is the electronic Hamiltonian and H^{SB} is the electron-nuclear coupling. We quantitatively illustrate this connection via exact simulations of a Hubbard-Holstein molecule using the Hierarchical Equations of Motion that show that increasing the degree of electronic interactions can enhance or suppress the rate of electronic coherence loss.

Published in: A. Kar, L. Chen, and I. Franco, J. Phys. Chem. Lett. **7**, 1616 (2016).

* ignacio.franco@rochester.edu

Understanding the behavior of electrons in matter is fundamental to our ability to characterize, design and control the properties of molecules and materials [1, 2]. Electronic correlations [3, 4] and decoherence [5–7] are two basic properties that are ubiquitously used to characterize the nature and quality of electronic quantum states. Correlations among electrons arise due to their pairwise Coulombic interactions, that lead to a dependency of the motion of an electron with that of other surrounding electrons. These correlations determine the energetic properties of electrons in matter and the character of their energy eigenstates [8, 9]. In turn, decoherence in molecules typically arises due to the interactions of the electrons with the nuclear degrees of freedom [10–12]. The nuclei act as an environment that induces a loss of phase relationship between quantum electronic states. Establishing mechanisms for electronic decoherence is central to our understanding of the excited state dynamics of molecules [13–16], to the development of useful approximations to model correlated electron-nuclear dynamics [17, 18], and to the design of strategies to preserve electronic coherence that can subsequently be exploited in quantum technologies [19, 20].

While electronic correlation and decoherence have been amply investigated separately, the connection between the two, if any, is not understood. This is partially due to the fact that usual definitions of electronic correlation, such as correlation energy [21] or natural occupation numbers [22], are only applicable to pure electronic systems [23, 24] and do not allow addressing this fundamental question. For this reason, it is unclear if decoherence can induce changes in correlation and, conversely, if correlations can modify the coherence content of a quantum state.

Here we demonstrate that electronic correlation and decoherence are coupled physical phenomena that need to be considered concurrently. We do so by extending the concept of electronic correlation to open non-equilibrium quantum systems, and showing that electronic correlation modulates the degree of entanglement between electrons and nuclei, and thus the degree of electronic decoherence. Conversely, we also show that the electronic decoherence modulates the degree of electronic correlation, as evidenced by the correlation energy. Further, we isolate conditions under which electronic correlations and decoherence can be considered as uncoupled physical phenomena and show that they are generally violated by molecules and materials, demonstrating that the connection between electronic correlation and decoherence is ubiquitous in matter. These formal developments are quantitatively illustrated via numerically exact computations in a Hubbard-Holstein molecule that

show that increasing the electronic interactions can strongly modulate the rate of electronic coherence loss.

To proceed, consider a pure electron-nuclear system with Hamiltonian $\mathcal{H} = H^S + H^B + H^{SB}$, where H^S is the electronic Hamiltonian, H^B the nuclear component, and H^{SB} the electron-nuclear couplings. Here, H^{SB} is defined as the residual electron-nuclear interactions that arise when the nuclear geometry deviates from a given reference configuration (e.g., the optimal geometry). The electronic Hamiltonian $H^S = H_0^S + V^S$ can be further decomposed into single-particle contributions H_0^S (e.g. Hartree-Fock) and residual two-body terms V^S. The latter arise from Coulombic interactions that cannot be mapped into one-body terms and introduce correlations among the electrons. The associated non-interacting Hamiltonian is obtained when $V^S = 0$, and is given by $\mathcal{H}_0 = H_0^S + H^B + H^{SB}$.

To extend the concept of electronic correlations to open non-equilibrium quantum systems, we require a correlation metric and a reference uncorrelated state for each electron-nuclear state. To construct the reference state, we imagine a fictitious process where for each physical time t the V^S term in the Hamiltonian is turned off adiabatically slow along a fictitious time coordinate τ (see Fig. S1 in the Supporting Information (SI)). Specifically, we suppose that the Hamiltonian of the system is of the form

$$\mathcal{H}_\epsilon(\tau) = \mathcal{H} - e^{-\epsilon|\tau|}V^S \quad (\epsilon > 0), \tag{1}$$

where the second term is considered as a perturbation to the $\mathcal{H}$-induced evolution. The physical evolution along t occurs at the $\tau = \tau_0 \to -\infty$ limit of the (t, τ) space for which the Hamiltonian is in its fully interacting form $\mathcal{H}_\epsilon(\tau_0) = \mathcal{H}$. In this limit, the state of the fully interacting system is given by

$$\hat{\rho}(t) = \sum_{i,j} \alpha_i(t)\alpha_j^*(t)|\psi_i\rangle\langle\psi_j|, \tag{2}$$

where $|\psi_i\rangle$ are eigenstates of $\mathcal{H}$ ($\mathcal{H}|\psi_i\rangle = E_i|\psi_i\rangle$). The uncorrelated reference state is generated by adiabatically turning off, in the Interaction picture, the V^S term in the Hamiltonian in the $\tau = \tau_0$ to $\tau = 0$ interval, i.e.

$$\hat{\rho}^{\mathrm{u}}(t) = \lim_{\epsilon\to 0}\lim_{\tau_0\to-\infty} U_{\epsilon I}(0,\tau_0)\hat{\rho}(t)U_{\epsilon I}^\dagger(0,\tau_0), \tag{3}$$

where $U_{\epsilon I}(\tau, \tau')$ is the evolution operator in Interaction picture. The latter is defined by the

Dyson series [4] $U_{\epsilon I}(\tau,\tau') = \mathbb{I} + \sum_{n=1}^{\infty} U_{\epsilon I}^{(n)}(\tau,\tau')$, where

$$U_{\epsilon I}^{(n)}(\tau,\tau') = -\frac{i}{\hbar}\int_{\tau'}^{\tau} d\tau_n e^{-\epsilon|\tau_n|} V_I(\tau_n) U_{\epsilon I}^{(n-1)}(\tau_n,\tau'),$$

$V_I(\tau) = -U_0^{\dagger}(\tau)V^S U_0(\tau)$ is the $-V^S$ operator in Interaction picture, and $U_0(\tau) = e^{-\frac{i}{\hbar}\mathcal{H}\tau}$ is the perturbation-free evolution operator.

Equation (3) captures changes in $\hat{\rho}(t)$ that are generated by the process of turning off V^S in the presence of a nuclear environment. It has the desirable property that $\hat{\rho}^{\mathrm{u}}(t) = \hat{\rho}(t)$ when $V^S = 0$, and it reduces to the usual adiabatic connection for isolated electronic systems when $H^{SB} = 0$. Note that we have chosen $U_{\epsilon I}(\tau)$ instead of the full evolution operator $U(\tau) = U_0(\tau)U_{\epsilon I}(\tau)$ to generate the uncorrelated states. This is because the $U_0(\tau)$ component of $U(\tau)$ leads to changes in $\hat{\rho}(t)$ due to electron-nuclear entanglements that are present even when $V^S = 0$. By contrast, $U_{\epsilon I}(\tau)$ solely captures electron-nuclear entanglements that can be modulated by the electron-electron interactions.

Switching off interactions adiabatically generates exact eigenstates of the non-interacting system from those of the interacting system via the Gell-Mann and Low theorem (GMLT) [1, 4]. The GMLT states that given an eigenstate $|\psi_i\rangle$ of the interacting $\mathcal{H}$, if the limit

$$\lim_{\epsilon\to 0} |\phi_i^{\epsilon}\rangle = \lim_{\epsilon\to 0} A_i^{-1} U_{\epsilon I}(0,-\infty)|\psi_i\rangle, \tag{4}$$

(where $A_i = \langle\psi_i|U_{\epsilon I}(0,-\infty)|\psi_i\rangle / |\langle\psi_i|U_{\epsilon I}(0,-\infty)|\psi_i\rangle|$ and $|A_i|^2 = 1$ because the $|\phi_i\rangle$ are chosen to be normalized) exists, then $\lim_{\epsilon\to 0}|\phi_i^{\epsilon}\rangle = |\phi_i\rangle$ is an eigenstate of the non-interacting $\mathcal{H}_0$. Applying the GMLT in Eq. (3) we arrive at the uncorrelated reference state that corresponds to $\hat{\rho}(t)$ in Eq. (2),

$$\hat{\rho}^{\mathrm{u}}(t) = \sum_{i,j} \alpha_i(t)\alpha_j^*(t) e^{i(\theta_i-\theta_j)} |\phi_i\rangle\langle\phi_j|. \tag{5}$$

Here, we have assumed that $\lim_{\epsilon\to 0} A_i A_j^{\star} = e^{i(\theta_i-\theta_j)}$ exists even when the phase factors $A_i \sim e^{\frac{i}{\epsilon}}$ are known to be ill-behaved as $\epsilon \to 0$ [4]. While the A_i introduce convergence issues at the wavefunction level, observable quantities, including the density operator, should remain finite during the unitary evolution.

As a physical measure of electronic correlation in electron-nuclear systems we choose the energetic difference between the correlated and uncorrelated state:

$$E_{\mathrm{cor}}(t) = \mathrm{Tr}[\hat{\rho}(t)\mathcal{H}] - \mathrm{Tr}[\hat{\rho}^{\mathrm{u}}(t)\mathcal{H}_0]. \tag{6}$$

This quantity measures energetic changes in the electron-nuclear system that are introduced by the process of turning off V^S during the adiabatic connection in Eq. (3), and parallels a common metric for correlation [21] used in closed electronic systems. Note that any energetic measure of correlation based on the properties of the electronic subsystem alone is not appropriate since it will unavoidably include relaxation channels due to interactions with the bath. Further note that definitions of correlation based on the non-idempotency of the single-particle electronic density matrix [22, 25] are not applicable since the non-idempotency can arise due to correlation or due to decoherence [26]. (see Ref. [27, 28] for measures claimed to operate in open quantum systems).

As a basis-independent measure of decoherence we employ the purity $P(t) = \mathrm{Tr}[\hat{\rho}_e^2(t)]$ where $\hat{\rho}_e(t) = \mathrm{Tr}_B[\hat{\rho}(t)]$ is the N-body electronic density matrix obtained by performing a partial trace over the nuclear bath. The purity $P = 1$ for pure states and $P < 1$ for mixed states. For pure electron-nuclear systems, the decoherence of the electronic (or nuclear) subsystem is solely due to electron-nuclear entanglement. Thus, in this regime, the decay of P also measures the degree of electron-nuclear entanglement.

In this context, it is now readily seen why correlation and decoherence are strongly connected. For this, first note that the coherence content of $\hat{\rho}_e(t)$ and $\hat{\rho}_e^{\mathrm{u}}(t)$ are generally different. To see this, consider $\hat{\rho}(t) = |\Psi(t)\rangle\langle\Psi(t)|$ in Eq. (2) for which $|\Psi(t)\rangle = \sum_i \alpha_i(t)|\psi_i\rangle$. In light of the Schmidt decomposition [20], $|\Psi(t)\rangle$ can be written as $|\Psi(t)\rangle = \sum_i \sqrt{\lambda_i(t)}|s_i(t)\rangle|b_i(t)\rangle$, where $|s_i(t)\rangle$ and $|b_i(t)\rangle$ are, respectively, orthonormal electron and nuclear states, and $\sqrt{\lambda_i}$ are the Schmidt coefficients ($\sum_i \lambda_i = 1, \lambda_i > 0$). In the Schmidt basis,

$$\hat{\rho}(t) = \sum_{i,j} \sqrt{\lambda_i \lambda_j}|s_i\rangle|b_i\rangle\langle b_j|\langle s_j|. \tag{7}$$

In terms of $\{\lambda_i\}$, the purity of the electronic (or nuclear) subsystem is $P(t) = \sum_i \lambda_i^2(t)$. In turn, the uncorrelated state $\hat{\rho}^{\mathrm{u}}(t) = |\Phi(t)\rangle\langle\Phi(t)|$ (Eq. (5)) is associated with $|\Phi(t)\rangle \equiv \sum_i \alpha_i(t)e^{i\theta_i}|\phi_i\rangle$. Under the Schmidt decomposition, $|\Phi(t)\rangle = \sum_i \sqrt{\mu_i(t)}|S_i(t)\rangle|B_i(t)\rangle$ and the resulting purity is $P^{\mathrm{u}}(t) = \sum_i \mu_i^2(t)$. Since $|\Phi(t)\rangle \neq |\Psi(t)\rangle$, the set $\{\mu_i\}$ is different from the set $\{\lambda_i\}$ and therefore the purity for the correlated state and its reference uncorrelated counterpart generally differ. That is, for $H^{SB} \neq 0$, V^S modulates the degree of coherence of electronic states.

Consider now the influence of H^{SB} on the correlation energy [Eq. (6)],

$$E_{\rm cor}(t) = \sum_i |\alpha_i(t)|^2 (E_i - \mathcal{E}_i), \tag{8}$$

where $\mathcal{H}|\psi_i\rangle = E_i|\psi_i\rangle$ and $\mathcal{H}_0|\phi_i\rangle = \mathcal{E}_i|\phi_i\rangle$. For $V^S \neq 0$, $E_{\rm cor}$ will change if H^{SB} changes because E_i and $\mathcal{E}_i$ vary differently as H^{SB} is modified. That is, H^{SB} influences $E_{\rm cor}$ because it modulates the response of the electron-nuclear system to V^S.

Decoherence and correlation decouple when

$$[H^S, H^{SB}] = 0, \tag{9}$$

for $V^S \neq 0$. When Eq. (9) holds, the H^{SB} does not introduce electronic relaxation and the system-bath dynamics is pure dephasing. To see how this sufficient condition arises, consider the decoherence case first. For the purity of $\hat{\rho}_e(t)$ and $\hat{\rho}_e^{\rm u}(t)$ to coincide, the evolution operator in Eq. (3) must not change the degree of entanglement between electrons and nuclei. For this to happen, $U_{\epsilon I}$ must be of the form

$$U_{\epsilon I}(0, -\infty) = U_{\epsilon I}^S(0, -\infty) \otimes \mathbb{I}^B, \tag{10}$$

where $U_{\epsilon I}^S$ is a purely electronic operator and $\mathbb{I}^B$ is the identity operator in the nuclear Hilbert space. Under these conditions, and in light of Eq. (7), $\hat{\rho}^{\rm u}(t) = \sum_{i,j} \sqrt{\lambda_i \lambda_j} |s_i'\rangle|b_i\rangle \otimes \langle b_j|\langle s_j'|$, where $|s_i'\rangle\langle s_j'| = \lim_{\epsilon\to 0} U_{\epsilon I}^S(0,-\infty)|s_i\rangle\langle s_j| U_{\epsilon I}^{S\,\dagger}(0,-\infty)$. Since the Schmidt coefficients for $\hat{\rho}^{\rm u}(t)$ are the same as those of $\hat{\rho}(t)$ (*cf.* Eq. (7)) the purity of the two states is identical. For $U_{\epsilon I}$ to be of the form in Eq. (10), $V_I(\tau)$ must be a purely electronic operator, i.e. $V_I(\tau) = \hat{O}^S(\tau) \otimes \mathbb{I}^B$, where $\hat{O}^S$ is an operator in the Hilbert space of the electronic subsystem. This is guaranteed when Eq. (9) is satisfied. Specifically,

$$V_I(\tau) = -e^{i\frac{\tau}{\hbar}H^S} e^{i\frac{\tau}{\hbar}(H^B + H^{SB})} V^S e^{-i\frac{\tau}{\hbar}(H^B + H^{SB})} e^{-i\frac{\tau}{\hbar}H^S},$$

where we have used the fact that $[H^S, H^B] = 0$ and the condition in Eq. (9). We arrive at the desired form

$$V_I(\tau) = -e^{i\frac{\tau}{\hbar}H^S} V^S e^{-i\frac{\tau}{\hbar}H^S} \otimes \mathbb{I}^B = \hat{O}^S(\tau) \otimes \mathbb{I}^B, \tag{11}$$

by taking into account that $[V^S, H^B] = 0$, and the fact that $[V^S, H^{SB}] = 0$ for Coulombic systems since V^S and H^{SB} are both functions of the position operators.

The correlation energy also becomes independent of H^{SB} when the commutation relations in Eq. (9) are satisfied. To show this, we contrast $E_{\rm cor}$ with the correlation energy $E_{\rm cor}^{(0)}$ that

would have been obtained if H^{SB} is not allowed to influence the response of the system as V^S is adiabatically turned off in Eq. (3). Specifically,

$$E^{(0)}_{\rm cor}(t) = {\rm Tr}[\hat{\rho}(t)\mathcal{H}] - {\rm Tr}[\hat{\rho}^{\rm u}_{(0)}(t)\mathcal{H}_0], \tag{12}$$

where the reference state $\hat{\rho}^{\rm u}_{(0)}(t) = \lim_{\tau_0\to-\infty,\epsilon\to 0}\left[U'_{\epsilon I}(0,\tau_0)\hat{\rho}(t)U'^{\dagger}_{\epsilon I}(0,\tau_0)\right]$ is obtained by setting $H^{SB}=0$ throughout the adiabatic process, i.e. $U'_{\epsilon I}(0,-\infty) = U_{\epsilon I}(0,-\infty)|_{H^{SB}=0}$. The interaction potential $V'_I(\tau)$ in $U'_{\epsilon I}(t,-\infty)$ is given by

$$V'_I(\tau) = V_I(\tau)|_{H^{SB}=0} = -e^{i\frac{\tau}{\hbar}H^S}V^S e^{-i\frac{\tau}{\hbar}H^S}\otimes\mathbb{I}^B \tag{13}$$

where we have used the fact that $[H^S, H^B] = [V^S, H^B] = 0$. If $E_{\rm cor}(t) = E^{(0)}_{\rm cor}(t)$ the correlation energy is independent of H^{SB}. For this to happen, the identity $V_I(\tau) = V'_I(\tau)$ must be satisfied such that $\hat{\rho}^{\rm u}_{(0)}(t)$ and $\hat{\rho}^{\rm u}(t)$ coincide. Since $V'_I(\tau)$ is identical to the limiting $V_I(\tau)$ in Eq. (11), by the same argument employed to arrive at Eq. (11) we conclude that $E_{\rm cor}(t) = E^{(0)}_{\rm cor}(t)$ when Eq. (9) is true.

From the perspective of the correlation energy, when Eq. (9) is satisfied $E_{\rm cor}$ is purely determined by the electronic subsystem. This is because $\langle H^{SB} + H^B\rangle$ remains constant as V^S is turned off adiabatically (as can be seen by writing the Heisenberg equations of motion for $H^{SB} + H^B$). From the perspective of the purity, Eq. (9) guarantees that the effect of the bath will be the same for the correlated system and its uncorrelated counterpart, thus eliminating a possible V^S dependence in the decoherence dynamics. Note that even for stationary Born-Oppenheimer (BO) states it is not possible for decoherence and correlation to be uncoupled unless Eq. (9) is satisfied. This is because even when stationary BO states are not entangled, the corresponding uncorrelated state generally will be.

The pure dephasing condition [Eq. (9)] is generally violated by molecules and materials, indicating that the connection between electronic correlation and decoherence is ubiquitous in matter. Nevertheless, pure dephasing dynamics can arise when the frequencies associated with nuclear motion are far detuned from the electronic transitions such that the nuclear dynamics does not lead to electronic transitions in the correlated and uncorrelated system, as can be the case in semiconducting quantum dots [29, 30]. Under such conditions, $H^{SB} \approx \sum_n \hat{F}_n \otimes |E_n\rangle\langle E_n|$, where $\{|E_n\rangle\}$ are the eigenstates of H^S, and the $\hat{F}_n$ are nuclear operators defined such that $[V^S, H^{SB}] = 0$.

We now quantitatively illustrate this connection using a neutral two-site, two-electron, Hubbard-Holstein model with zero net spin as an example [1]; a minimal molecular model

that violates the commutation relations in Eq. (9) and satisfies $[V^S, H^{SB}] = 0$ as is expected for molecules. Here the electrons are described by the Hubbard Hamiltonian

$$H^S = -t_0 \sum_{\sigma\in\{\uparrow,\downarrow\}} (\hat{d}^\dagger_{1\sigma}\hat{d}_{2\sigma} + \hat{d}^\dagger_{2\sigma}\hat{d}_{1\sigma}) + U(\hat{n}_{1\uparrow}\hat{n}_{1\downarrow} + \hat{n}_{2\uparrow}\hat{n}_{2\downarrow}) \tag{14}$$

where $\hat{d}^\dagger_{i\sigma}$ (or $\hat{d}_{i\sigma}$) creates (or annihilates) an electron on site i with spin σ and satisfies the usual anticommutation relations $\{\hat{d}_{i\sigma}, \hat{d}^\dagger_{j\sigma'}\} = \delta_{i,j}\delta_{\sigma,\sigma'}$. The quantity $\hat{n}_{i\sigma} = \hat{d}^\dagger_{i\sigma}\hat{d}_{i\sigma}$ is the number operator, t_0 is the hopping parameter, and U is the energy penalty for having two electrons on the same site. The Hubbard Hamiltonian can be decomposed into a Hartree-Fock component $H^S_0 = -t_0 \sum_{\sigma\in\{\uparrow,\downarrow\}}(\hat{d}^\dagger_{1\sigma}\hat{d}_{2\sigma} + \hat{d}^\dagger_{2\sigma}\hat{d}_{1\sigma}) + 2U\sum_{i,\sigma}\hat{n}_{i\sigma}\langle\hat{n}_{i,-\sigma}\rangle - U\sum_{i,\sigma}\langle\hat{n}_{i\sigma}\rangle\langle\hat{n}_{i,-\sigma}\rangle$, and a two-body term $V^S = H^S - H^S_0$, where the expectation value $\langle\hat{n}_{i\sigma}\rangle = 1/2$ is over the equilibrium thermal state. The nuclei are described as four baths of N^m_b harmonic oscillators, with Hamiltonian

$$H^B = \sum_{m=1}^{4}\sum_{j=1}^{N^m_b}\left(\frac{p^2_{mj}}{2} + \frac{1}{2}\omega^2_{mj}x^2_{mj}\right), \tag{15}$$

where x_{mj} is the mass-weighted displacement away from equilibrium for the jth harmonic oscillator in the mth harmonic bath, p_{mj} is the momentum conjugate to x_{mj} and ω_{mj} its oscillation frequency. We assume that each set of harmonic oscillators couples to an independent electronic configuration of zero net spin. Specifically, we choose

$$H^{SB} = F_1\hat{n}_{1\uparrow}\hat{n}_{1\downarrow} + F_2\hat{n}_{2\uparrow}\hat{n}_{2\downarrow} + F_3\hat{n}_{1\uparrow}\hat{n}_{2\downarrow} + F_4\hat{n}_{1\downarrow}\hat{n}_{2\uparrow}, \tag{16}$$

where $F_m = \sum_{j=1}^{N^m_b} c_{mj}x_{mj}$ is a collective bath coordinate of bath m. The effective electron-nuclear coupling is specified by the spectral density $J_m(\omega) = \frac{\pi}{2}\sum_{j=1}^{N^m_b}\frac{c^2_{mj}}{\omega_{mj}}\delta(\omega - \omega_{mj})$ which is assumed to be same for all the states and of Debye form $J(\omega) = \eta\frac{\gamma\omega}{\omega^2+\gamma^2}$. Here γ is the characteristic frequency of the bath and the parameter η effectively determines the electron-nuclear coupling strength.

The electronic dynamics generated by this model is propagated exactly using the Hierarchical Equations of Motion approach [31–34], a non-perturbative and non-Markovian theory of reduced system dynamics. As an initial state, we consider a separable electron-nuclear state $\hat{\rho}(0) = \hat{\rho}_e(0) \otimes \hat{\rho}_n(0)$ where the nuclei are initially at thermal equilibrium $\hat{\rho}_n(0) = \exp(-\beta H^B)/\mathrm{Tr}_B\{\exp(-\beta H^B)\}$ with inverse temperature β, and the electrons $\hat{\rho}_e(0) = |\Psi\rangle\langle\Psi|$ in a superposition $|\Psi\rangle = \frac{1}{\sqrt{2}}(|E_1\rangle + |E_2\rangle)$ between the ground and first excited state.

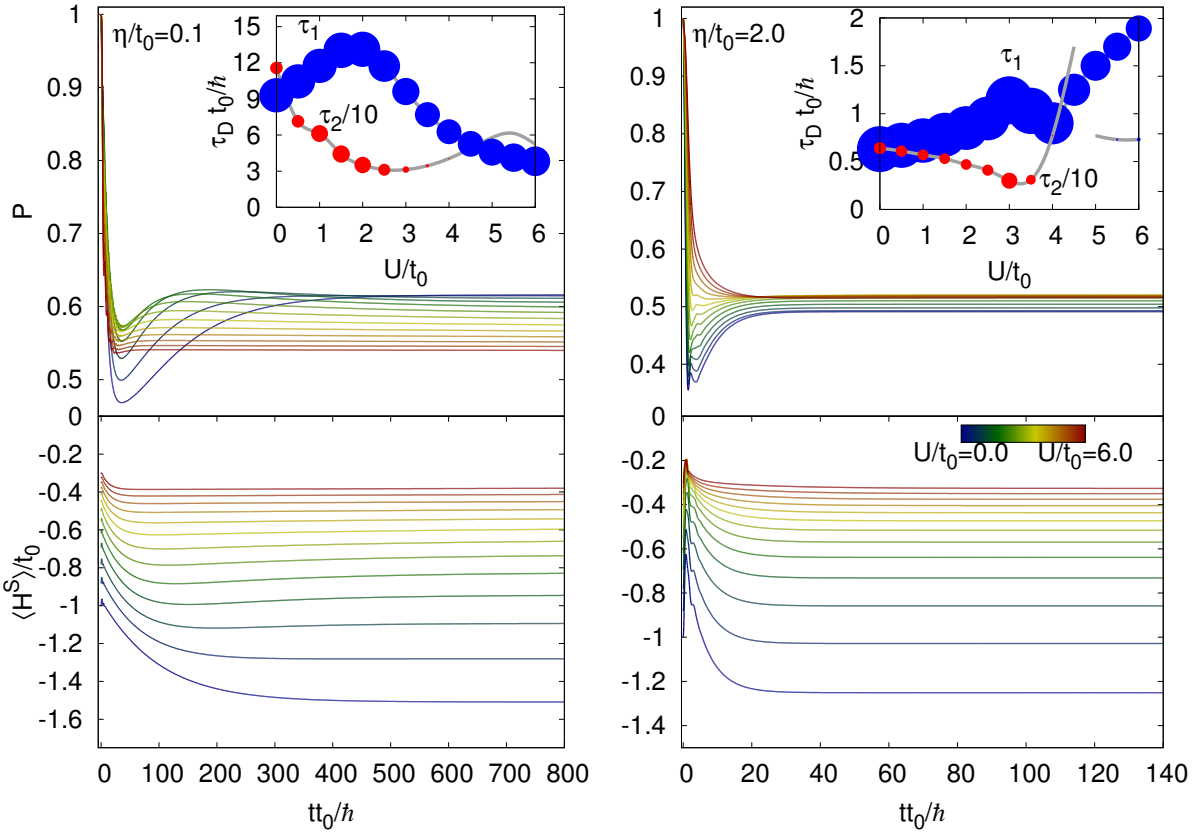

FIG. 1: Purity and electronic energy during the evolution of the Hubbard-Holstein molecule ($\beta = 1/t_0, \hbar\gamma = 0.3t_0$). The inset shows characteristic timescales in $P(t)$ obtained from an exponential fit $P - P_{\text{thermal}} = \sum_{i=1}^{3} a_i \exp(-t/\tau_i)$, see SI. The dot size measures the magnitude of $|a_i|$ (blue, $a_i > 0$; red, $a_i < 0$; a_3 is small and not shown). Note how increasing U can enhance or suppress the decoherence.

Figure 1 shows the dynamics of the purity and the electronic energy for different electronic interactions U and effective electron-nuclear couplings η (inset: characteristic decay timescales τ_i in $P(t)$). The fact that Eq. (9) is violated is reflected by the energetic relaxation of the electrons. The purity observes a sharp initial decay on a τ_1 timescale, followed by a slower dynamics on a τ_2 timescale that asymptotically leads the electronic subsystem to a state of thermal equilibrium. In the presence of electronic correlations, varying U strongly modulates the decoherence and relaxation dynamics. By contrast, in the Hartree-Fock approximation the purity for this model is independent of U and equal to the one for $U = 0$. For $U \leq 3t_0$ the decoherence is determined by τ_2. In turn, for $U \geq 4t_0$ the importance of τ_2 in the dynamics (as characterized by the dot sizes in Fig. 1) is diminished, and the

decoherence time is determined by τ_1. *Note how increasing U can enhance or suppress the rate of electronic decoherence.* Specifically, for $\eta = 0.1t_0$, increasing U leads to a decrease in the decoherence time. By contrast, for $\eta = 2.0t_0$, increasing U leads to a decrease followed by an increase in the decoherence time. As expected, the rate of decoherence is faster in the stronger η case.

The molecular mechanisms at play in Fig. 1 can be identified by examining the effect of changing η and U on the potential energy surfaces (PESs). As detailed in the SI, increasing U brings the ground and first excited state closer together in energy, and reduces the difference in curvature between their PESs. The first effect increases the decoherence rate because it increases the nonadiabatic couplings between the two states. Excitation by an incoherent bath leads to decoherence [35]. Thus, the enhanced excitation of the electrons by the *thermal* nuclei increases the decoherence rate. The second effect, by contrast, slows down the decoherence. To see this, recall that for a general vibronic state $|\Psi\rangle = \sum_n |E_n\rangle|\chi_n\rangle$ the electronic density matrix is given by $\hat{\rho}_e = \sum_{nm}\langle\chi_m|\chi_n\rangle|E_n\rangle\langle E_m|$. The coherences between states $|E_n\rangle$ and $|E_m\rangle$ are thus determined by the nuclear wavepacket overlap $S_{mn} = \langle\chi_m|\chi_n\rangle$ [12, 36]. By making the PESs look more alike, increasing U slows down the decay of S_{mn} for each member of the initial ensemble due to wavepacket evolution in alternative PESs. It is the non-trivial competition between these two effects what leads to the intricate dynamics in Fig. 1.

Note that the nonadiabatic couplings between the ground (singlet) and first excited (triplet) state that are responsible for the first decoherence mechanism arise due to the $F_3\hat{n}_{1\uparrow}\hat{n}_{2\downarrow}$ and $F_4\hat{n}_{1\downarrow}\hat{n}_{2\uparrow}$ terms in H^{SB}. By contrast, the second decoherence mechanism is determined by all four terms in H^{SB} and survives even in the absence of singlet-triplet couplings. In this limit, increasing U protects the electrons from the decoherence.

Does decoherence help us reduce the complexity of the many-body electron problem? Figure 2 shows the evolution of the two-particle cumulant ($\mathrm{Tr}[\lambda_2] = \mathrm{Tr}[{}^{(1)}\Gamma^2 - {}^{(1)}\Gamma]$, where ${}^{(1)}\Gamma$ is the 1-body electronic density matrix) which measures the importance of 2-body contributions to $\hat{\rho}_e$ that cannot be decomposed in terms of ${}^{(1)}\Gamma$ [25]. For an uncorrelated closed electronic system ${}^{(1)}\Gamma^2 = {}^{(1)}\Gamma$ and $\mathrm{Tr}[\lambda_2] = 0$. As shown, instead of reducing the complexity, in this case increasing η (and U) enhances the importance of higher order r-body electronic density matrices to the BBGKY hierarchy [37].

In conclusion, we have shown that the correlation among electrons and the degree of

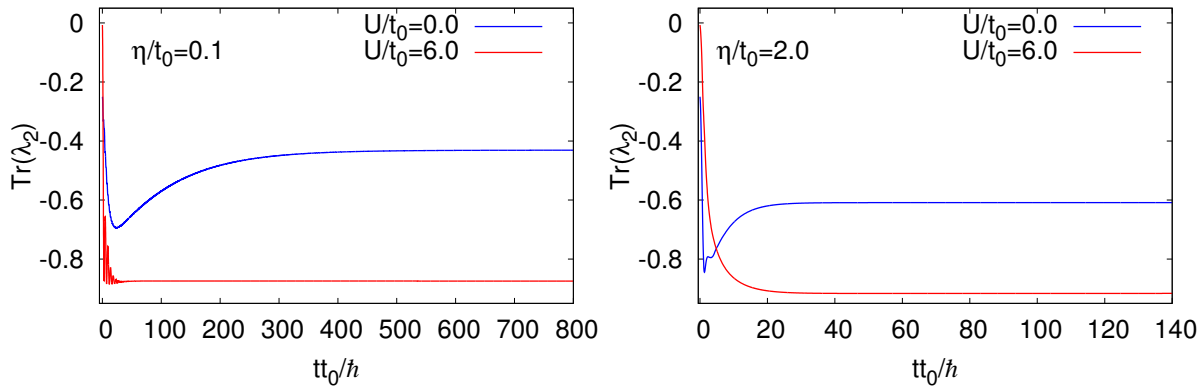

FIG. 2: Two-particle cumulant during the evolution in Fig. 1.

quantum coherence of electronic states are strongly coupled in matter. For arbitrary states, only when the system-bath dynamics is pure dephasing such that Eq. (9) is satisfied can correlation and decoherence be considered as uncoupled physical phenomena. Investigating the consequences of this fundamental, ubiquitous, and previously overlooked connection constitutes an emerging challenge in electronic structure and molecular dynamics.

ACKNOWLEDGEMENT

This material is based upon work supported by the National Science Foundation under CHE - 1553939. I.F. thanks Prof. John Parkhill for helpful discussions.

SUPPORTING INFORMATION AVAILABLE

The Supporting Information includes plots for the evolution of the electronic density matrix, the PESs for representative examples, and a discussion of the mechanisms at play in Fig. 1.

Understanding the Fundamental Connection Between Electronic Correlation and Decoherence: Supporting Information

I. SCHEME OF THE ADIABATIC CONNECTION IN EQS. (1)-(5)

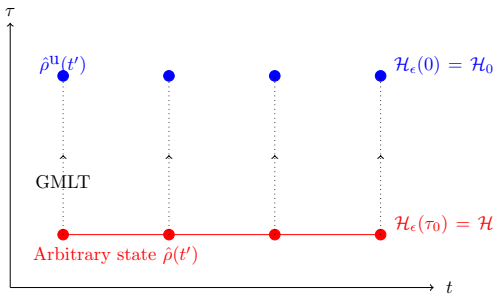

FIG. S1: At each instant of time t, the uncorrelated counterpart $\hat{\rho}^{\mathrm{u}}(t)$ of a general electron-nuclear state $\hat{\rho}(t)$ can be obtained by turning off the residual electron-electron interactions V^S adiabatically slow via evolution in the Interaction picture along a fictitious time coordinate τ.

II. DECOHERENCE DYNAMICS OF THE HUBBARD-HOLSTEIN MODEL

To clarify the molecular mechanisms at play in the decoherence dynamics of the Hubbard-Holstein model shown in Fig. 1, below we discuss the effect of changing U and η on the electronic potential energy surfaces (PESs) and on the dynamics of the electronic density matrix.

A. Dynamics of the electronic density matrix $\hat{\rho}_e(t)$

Figure S2 shows the dynamics of $\hat{\rho}_e(t)$ in the eigenbasis of H^S for four representative cases ($U = 0t_0, 6t_0$; $\eta = 0.1t_0, 2.0t_0$). The characteristic relaxation timescale of each matrix element was obtained via an exponential fit and tabulated in Table S1. As can be seen from Figure S2 and Table S1, the most important diagonal elements of $\hat{\rho}_e(t)$ ($\hat{\rho}_e^{11}(t)$ and $\hat{\rho}_e^{22}(t)$) decay faster for $U = 6t_0$ than $U = 0t_0$ indicating that increasing the electron-electron

interactions generally leads to faster relaxation. For $\eta = 0.1t_0$, the decay of the initial coherence between the ground and first excited state $\hat{\rho}_e^{12}(t)$ is largely unaffected by varying U. By contrast, for $\eta = 2.0t_0$ the decay of $\hat{\rho}_e^{12}(t)$ is slower for $U = 6t_0$ than $U = 0t_0$ signaling that increasing U protects the coherences between these two electronic energy eigenstates. Naturally, the thermalization of $\hat{\rho}_e(t)$ is faster for the stronger electron-nuclear coupling ($\eta = 2.0t_0$) than for the weak electron-nuclear coupling ($\eta = 0.1t_0$). As described in the sections below, these features of the dynamics of $\hat{\rho}_e(t)$ can be understood by investigating the effect of changing U and η on the PESs,

Note that the characteristic decay timescales for $\hat{\rho}_e(t)$ in Table S1 are related to the decoherence timescales obtained from the purity (Table S2). This is because, the thermalization of the purity

$$P(t) = \mathrm{Tr}[\hat{\rho}_e^2(t)] = \sum_{i,j} |\hat{\rho}_e^{ij}(t)|^2, \tag{S1}$$

is determined by the individual contributions to the density matrix $\hat{\rho}_e^{ij}(t)$.

B. Effect of changing U and η on the PESs

Consider now the effect of changing U and η on the PESs of the Hubbard-Holstein model. For definitiveness, we focus on the limiting case where the molecule is coupled to just one of the harmonic oscillators in each independent bath. In this case, the Hubbard-Holstein model Eqs. (14)-(16) reduces to:

$$\begin{aligned}\mathcal{H} = &- t_0 \sum_{\sigma\in\{\uparrow,\downarrow\}} (\hat{d}_{1\sigma}^\dagger \hat{d}_{2\sigma} + \hat{d}_{2\sigma}^\dagger \hat{d}_{1\sigma}) + U(\hat{n}_{1\uparrow}\hat{n}_{1\downarrow} + \hat{n}_{2\uparrow}\hat{n}_{2\downarrow}) + \sum_{m=1}^{4} \left(\frac{p_m^2}{2} + \frac{1}{2}\omega^2 x_m^2\right) \\ &+ c_1 x_1 \hat{n}_{1\uparrow}\hat{n}_{1\downarrow} + c_2 x_2 \hat{n}_{2\uparrow}\hat{n}_{2\downarrow} + c_3 x_3 \hat{n}_{1\uparrow}\hat{n}_{2\downarrow} + c_4 x_4 \hat{n}_{1\downarrow}\hat{n}_{2\uparrow},\end{aligned} \tag{S2}$$

where the frequency is taken to be at the peak of the spectral density ($\hbar\omega = 0.3t_0$). The strength of the electron-nuclear coupling is determined by $\{c_m\}$, chosen to be $c_m = \omega\sqrt{\frac{\eta}{\pi}}$. While this system does not correspond exactly to the system that is modeled through the HEOM approach, it does allow extracting qualitative understanding of the effect of changing U and η on the PESs. Figure S3 shows one-dimensional projections of the four PESs for this model along x_2 (with $x_1 = x_3 = x_4 = 0$) and x_3 (with $x_1 = x_2 = x_4 = 0$) for different choices of U and η. Note that for this simplified model the PESs along x_3 and x_4 (or x_1

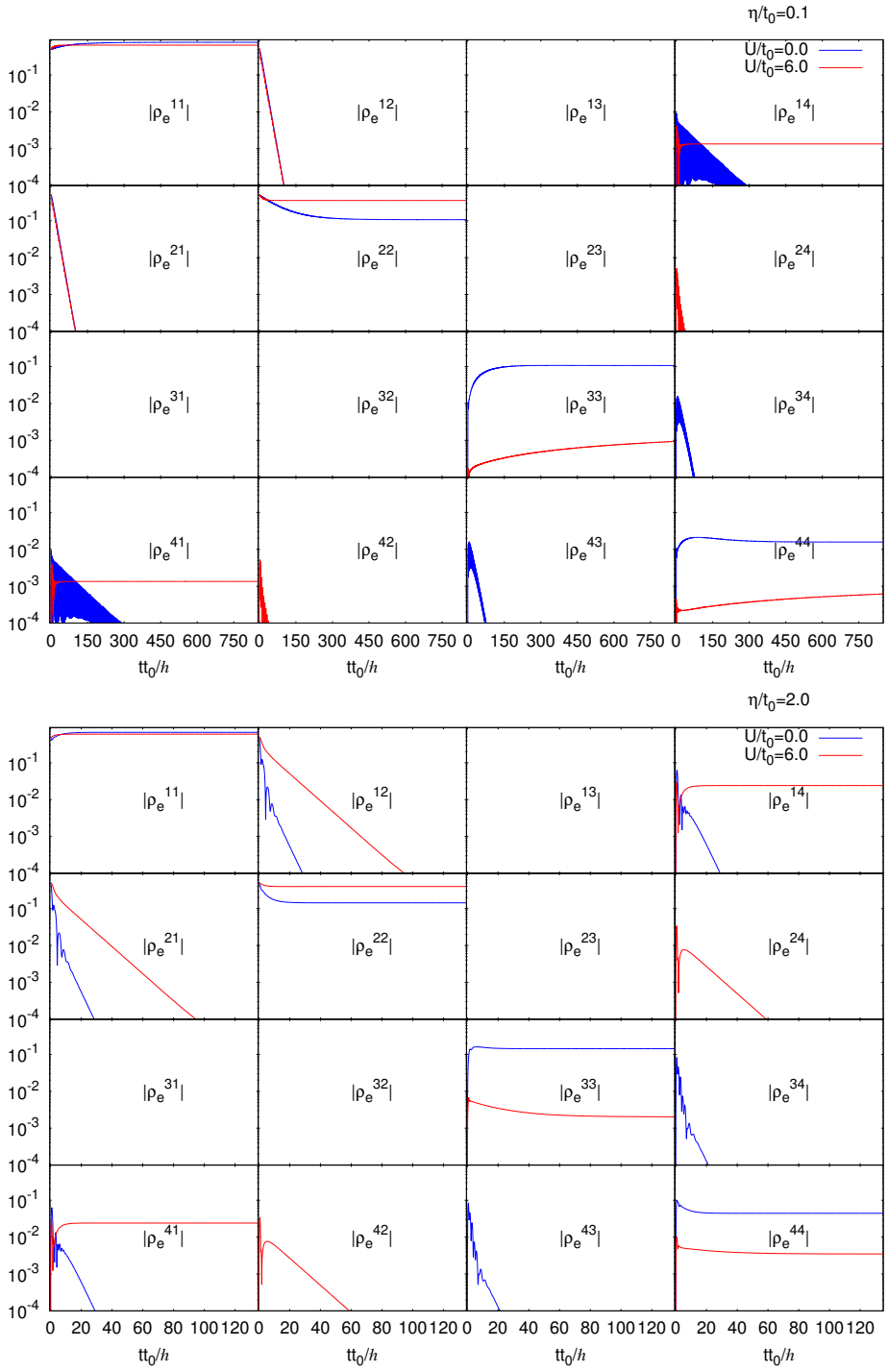

FIG. S2: Evolution of the electronic density matrix $\hat{\rho}_e(t)$ under the conditions in Fig. 1 with $\eta = 0.1t_0$ (top) and $\eta = 2.0t_0$ (bottom). Each panel corresponds to a different matrix element of $\hat{\rho}_e^{ij}(t) = \langle E_i|\hat{\rho}_e(t)|E_j\rangle$ in the eigenbasis of H^S $\{|E_i\rangle\}$ ordered with increasing energy. Initially $\hat{\rho}_e(0) = |\Psi\rangle\langle\Psi|$, where $|\Psi\rangle = \frac{1}{\sqrt{2}}(|E_1\rangle + |E_2\rangle)$. Timescales for the decay of $\hat{\rho}_e^{ij}(t)$ based on an exponential fit are shown in Table S1. Note that for $\eta = 2.0t_0$ the initial coherence between ground and first excited state ($\hat{\rho}_e^{12}(t)$) is protected by increasing U. By contrast, for $\eta = 0.1t_0$ the decay of $\hat{\rho}_e^{12}(t)$ is independent of U.

(a) $\eta/t_0 = 0.1$

	$U/t_0 = 0$		$U/t_0 = 6$	
	p	$\tau(t_0/\hbar)$	p	$\tau(t_0/\hbar)$
$\hat{\rho}_e^{11}$	-0.2763	92.42	-0.1568	11.65
$\hat{\rho}_e^{12}$	0.5449	12.82	0.4993	10.91
$\hat{\rho}_e^{13}$	0		0	
$\hat{\rho}_e^{14}$	0.0038	67.34	0	
$\hat{\rho}_e^{22}$	0.3861	80.12	0.1571	12.47
$\hat{\rho}_e^{23}$	0		0	
$\hat{\rho}_e^{24}$	0		0.0036	7.923
$\hat{\rho}_e^{33}$	-0.1055	63.45	-0.0018	1533
$\hat{\rho}_e^{34}$	0.0116	22.24	0	
$\hat{\rho}_e^{44}$	0.0032	319.5	-0.0009	1550

(b) $\eta/t_0 = 2.0$

	$U/t_0 = 0$		$U/t_0 = 6$	
	p	$\tau(t_0/\hbar)$	p	$\tau(t_0/\hbar)$
$\hat{\rho}_e^{11}$	-0.2633	6.134	-0.1162	3.025
$\hat{\rho}_e^{12}$	0.5289	1.244	0.4515	7.679
$\hat{\rho}_e^{13}$	0		0	
$\hat{\rho}_e^{14}$	0.0372	2.810	-0.0166	5.880
$\hat{\rho}_e^{22}$	0.3265	3.723	0.1146	2.616
$\hat{\rho}_e^{23}$	0		0	
$\hat{\rho}_e^{24}$	0		0.0112	13.75
$\hat{\rho}_e^{33}$	0.0009	123.8	0.0033	23.17
$\hat{\rho}_e^{34}$	0.0565	2.601	0	
$\hat{\rho}_e^{44}$	0.0343	7.220	0.0023	19.02

TABLE S1: Characteristic timescales in the thermalization of the density matrix of the Hubbard-Holstein model shown in Fig. S2. The data corresponds to an exponential fit of the decay $\hat{\rho}_e^{ij}(t) - \hat{\rho}_e^{ij}(\infty) = pe^{-\frac{t}{\tau}}$, where τ is the timescale and p its weight.

and x_2) coincide. As can be seen in Fig. S3, for weak electron-nuclear couplings ($\eta = 0.1t_0$) the 4 PESs are very similar, while for the stronger $\eta = 2.0t_0$ the minimum and curvature of the PESs generally differ. In both cases, the effect of increasing U is to bring the ground and first excited state (or second and third excited states) closer together in energy, and to reduce the difference in curvature of the PESs associated with the ground and first excited state.

The reduction in curvature difference can be quantified through

$$\langle \Delta F \rangle = \langle F_1 - F_2 \rangle = \frac{\sum_n e^{-\beta\epsilon_n} \langle \chi_n | (F_1 - F_2) | \chi_n \rangle}{\sum_n e^{-\beta\epsilon_n}}, \tag{S3}$$

which measures the average of the difference in the curvatures $F_n = dE^{(n)}(x_i)/dx_i$ between ground ($n = 1$) and first ($n = 2$) excited state along a particular nuclear coordinate x_i, where $E^{(n)}(x_i)$ is the adiabatic PES of the n-th electronic state along x_i. The average is taken over

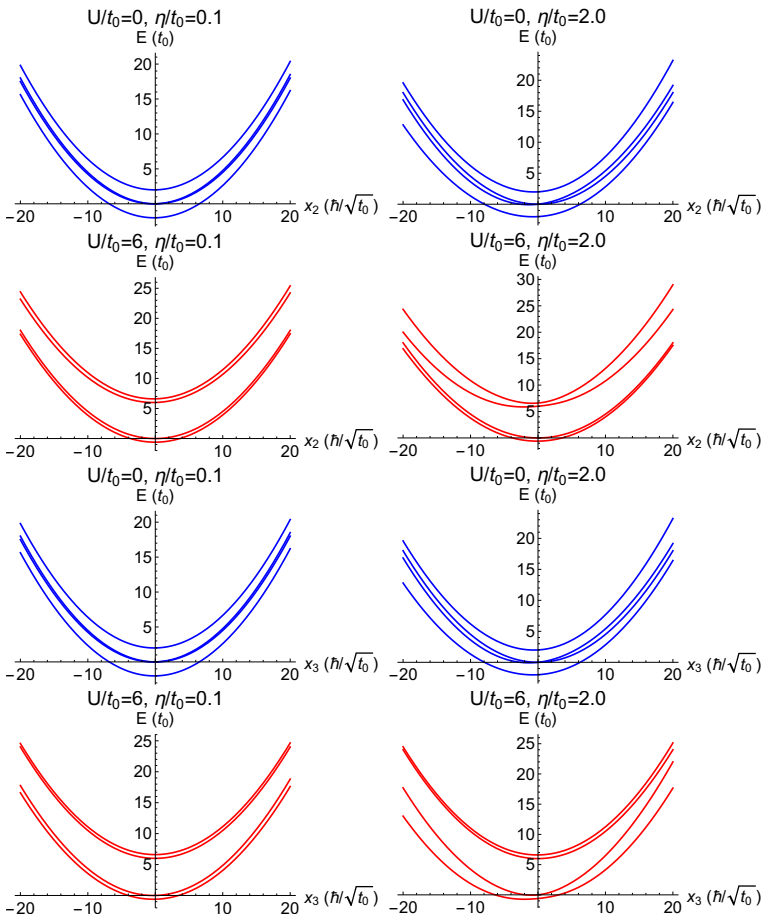

FIG. S3: Projections of the PESs for the simplified Hubbard-Holstein model defined in Eq. (S2) along x_2 (with $x_1 = x_3 = x_4 = 0$), $E^{(n)}(x_2)$, and x_3 (with $x_1 = x_2 = x_4 = 0$), $E^{(n)}(x_3)$, with $n = 1, \cdots, 4$. The PESs along x_4 (or x_1) are identical to those along x_3 (or x_2). Note that with an increase in U the ground and first excited (or second and third excited) states come closer in energy.

the initial nuclear thermal state, where ϵ_n and $|\chi_n\rangle$ are the eigenvalues and eigenfunctions of the n-th harmonic oscillator level, and β the inverse temperature. As shown in Fig. S4, increasing U generally leads to a decrease in the difference in curvature between the ground and first excited state along all nuclear directions. Note that the $\langle \Delta F \rangle$ for $\eta = 0.1t_0$ are ~ 5 times smaller than those for $\eta = 2.0t_0$.

The decrease in energy difference between the ground and first excited state with increasing U, causes the nonadiabatic couplings (NACs), d_{12}, between these two states to increase (see Fig. S5). The NACs between electronic eigenstates $|\phi_1(x_m)\rangle$ and $|\phi_2(x_m)\rangle$ are defined

by [38]

$$d_{12} = |\langle \phi_1(x_m)| \frac{\partial}{\partial x_m} |\phi_2(x_m)\rangle|. \tag{S4}$$

Here $|\phi_i(x_m)\rangle$ refers to the i-th Born-Oppenheimer (BO) electronic eigenstate of the Hamiltonian (obtained by diagonalizing everything in Eq. (S2) except the nuclear kinetic energy). The d_{12} measure the coupling between two electronic levels via nuclear motion. An increase in the NACs leads to increased excitation of the electrons via nuclear dynamics. As shown in Fig. S5, the NACs are ~ 5 times larger for the case of stronger electron-nuclear couplings. Further, the NACs increase significantly with an increase in U for both values of η considered as a result of the energy levels coming closer together.

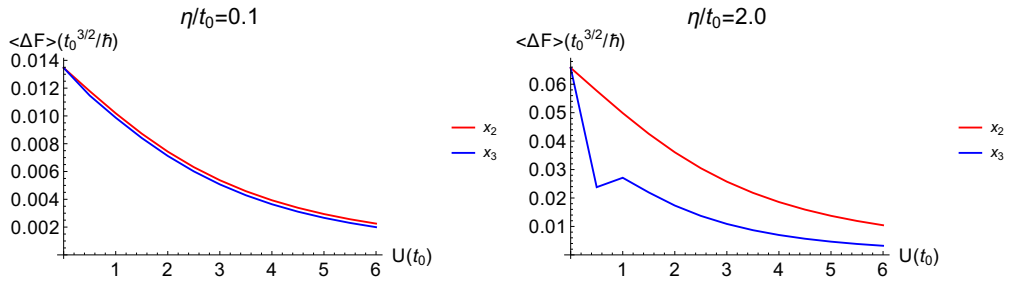

FIG. S4: Average of the difference in forces $\langle \Delta F \rangle$ (Eq. (S3)) between the ground and first excited state for different U and η along two different nuclear coordinates x_2 (with $x_1 = x_3 = x_4 = 0$) and x_3 (with $x_1 = x_2 = x_4 = 0$). The decrease in $\langle \Delta F \rangle$ with an increase in U can increase the lifetime of coherences between these two states.

C. Two competing decoherence mechanisms

As detailed above, increasing U brings the ground and first excited state closer together in energy, and reduces the difference in curvature between their PESs. As we now discuss, these two effects on the PESs lead to competing decoherence mechanisms that underlie the dynamics in Fig. 1.

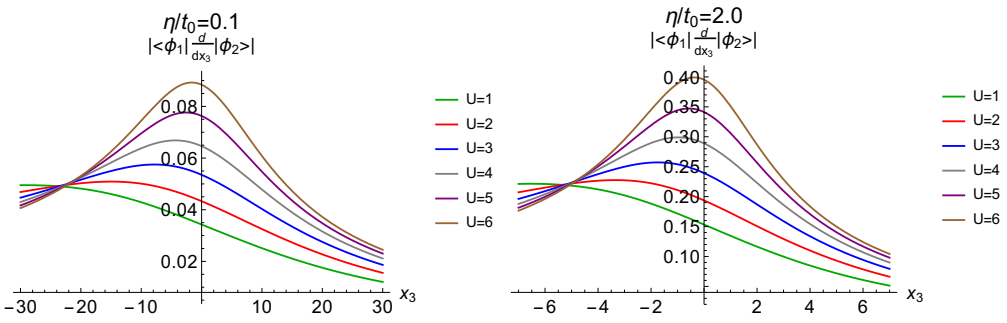

FIG. S5: Nonadiabatic couplings (NACs) [Eq. (S4)] between the ground ($|\phi_1\rangle$) and first excited BO electronic state ($|\phi_2\rangle$) as a function of the nuclear coordinate x_3 (or x_4) for $\eta = 0.1t_0$ (left) and $\eta = 2.0t_0$ (right). The NACs vanish along the nuclear coordinate x_1 and x_2. As U increases, $|\phi_1\rangle$ and $|\phi_2\rangle$ come closer in energy (see Fig. S3) causing an increase in the NACs.

1. Increasing U decreases the rate of decoherence because it reduces the difference in curvature between the PESs

In pure electron-nuclear systems, decoherence arises because of nuclear evolution in alternative PESs. To see this, consider the electronic density matrix associated with a general entangled vibronic state $|\Omega(t)\rangle = \sum_n |E_n\rangle|\chi_n(t)\rangle$,

$$\hat{\rho}_e(t) = \mathrm{Tr}_B\{|\Omega\rangle\langle\Omega|\} = \sum_{nm}\langle\chi_m(t)|\chi_n(t)\rangle|E_n\rangle\langle E_m|, \tag{S5}$$

where the trace is over the environmental degrees of freedom, the $\{|E_n\rangle\}$ are the eigenstates of H^S and the $|\chi_n(t)\rangle$ is the nuclear wavepacket associated with the n-th electronic state. Note that the coherences between electronic eigenstates (the off-diagonal elements in $\hat{\rho}_e(t)$) are determined by the nuclear overlaps $S_{nm}(t) = \langle\chi_m(t)|\chi_n(t)\rangle$. Thus, the loss of coherences in $\hat{\rho}_e(t)$ can be interpreted as the result of the decay of the S_{nm} during the coupled electron-nuclear evolution [12, 36]. Anything that leads to a decay in the nuclear overlaps (anharmonicities in the PES, nuclear motion in high-dimensional space, etc.) leads to decoherence. Standard measures of decoherence capture precisely this. For example, the purity, the measure of decoherence that we focus on here, is given by

$$P(t) = \sum_{nm}|\langle\chi_m(t)|\chi_n(t)\rangle|^2 \tag{S6}$$

and decays with the overlaps between the environmental states S_{nm}.

The effect of increasing U is to reduce the difference in the curvature between the ground and first excited state as revealed by $\langle \Delta F \rangle$ in Fig. S4. This effect is particularly important for $\eta = 2.0t_0$ while for $\eta = 0.1t_0$ the four PESs are very similar to one another even for $U = 0t_0$. Given the initial coherence between the ground and first excited state, this reduction in the curvature is expected to slow down the decoherence because it leads to a slower decay in the overlap of the nuclear wavepackets S_{12} associated with these two states for each member of the initial thermal ensemble. For $\eta = 2.0t_0$, this feature is clearly reflected in the dynamics of $\hat{\rho}_e^{12}(t)$ that shows an increase in coherence time from 1.2 to 7.7 $t_0/\hbar$ as U changes from $0t_0$ to $6t_0$ (Fig. S2). By contrast, for $\eta = 0.1t_0$, the shape of the PESs is mostly unaltered by varying U, hence the reason why in Fig. S2 the $\hat{\rho}_e^{12}(t)$ decay at approximately the same rate for $U = 0t_0$ and $U = 6t_0$.

2. Increasing U increases the rate of decoherence because it reduces the energy difference between electronic states

By reducing the energy difference between the ground and first excited state, increasing U introduces an additional decoherence mechanism in the dynamics that arises because the nuclei are initially prepared in a thermal incoherent state. Specifically, as the energy difference between levels is reduced with increasing U, the NACs between such levels increase (see Fig. S5). This increase in the coupling leads to an enhanced excitation of the electronic degrees of freedom by the nuclear dynamics. Now, excitation of a coherent system by an incoherent bath leads to decoherence [35]. Therefore, the enhanced excitation of the electronic subsystem by the thermal incoherent nuclear state leads to an increased rate of decoherence. For small U, the PESs in Fig. S3 are well separated in energy and this mechanism is suppressed. As U increases this mechanism becomes increasingly important leading to faster decoherence.

Note that for $\eta = 0.1t_0$ this mechanism is expected to be dominant since the PESs in this case are essentially parallel. This explains the comparatively long decoherence time observed when $U = 0t_0$. By contrast, for $\eta = 2.0t_0$ both decoherence mechanisms are expected to play a role. This explains why the decoherence is significantly faster for $\eta = 2.0t_0$ with respect to $\eta = 0.1t_0$ for all U considered.

III. TIMESCALES IN THE PURITY DYNAMICS

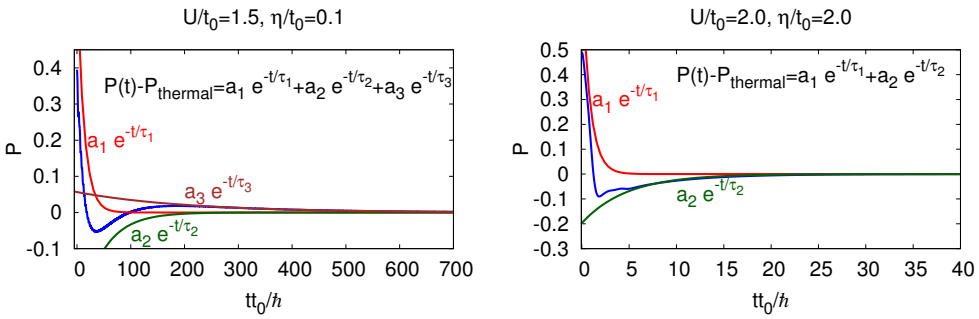

FIG. S6: Pictorial representation of the timescales associated with the purity dynamics for $\eta = 0.1t_0$ (left) and $\eta = 2.0t_0$ (right) is exemplified in a particular case. For $\eta = 0.1t_0$, the three timescales τ_1, τ_2, τ_3 can be associated with the initial decay, growth and final thermalization to thermal purity. For $\eta = 2.0t_0$, τ_1 captures the initial decay followed by a growth/decay captured by timescale τ_2.

Here we illustrate the meaning of the characteristic decoherence timescales τ_1 and τ_2 in Fig. 1 through a particular example. Figure S6 shows the three timescales τ_1, τ_2 and τ_3 associated with the purity dynamics obtained through a tri-exponential fit. The initial decay is captured by τ_1 which has a significant contribution to the purity (see Table S2), followed by a growth in purity captured by τ_2 and subsequently a final decay captured by τ_3. The contribution of the τ_3 timescale is negligible in the $\eta = 2.0t_0$ dynamics and quite small for $\eta = 0.1t_0$ (see Table S2), and is not included in Fig. 1.

TABLE S2: Characteristic timescales τ_i in the dynamics of the purity in Fig. 1 extracted from a triexponential fit $P(t) - P_{\text{thermal}} = \sum_{i=1}^{3} a_i \exp(-t/\tau_i)$, where a_i quantifies the weight of each contribution. Note that $a_3 = 0$ for $\eta = 2.0t_0$ and small for $\eta = 0.1t_0$.

(a) $\eta/t_0 = 0.1$

	$P(t) - P_{\text{thermal}} = \sum_{i=1}^{3} a_i \exp(-t/\tau_i)$					
U	a_1	$\tau_1(t_0/\hbar)$	a_2	$\tau_2(t_0/\hbar)$	a_3	$\tau_3(t_0/\hbar)$
$0.0t_0$	0.631	9.30	-0.232	115.71	0	
$0.5t_0$	0.631	10.45	-0.231	71.38	0	
$1.0t_0$	0.630	11.74	-0.310	61.24	0.076	148.85
$1.5t_0$	0.653	13.03	-0.318	44.19	0.056	204.12
$2.0t_0$	0.649	13.12	-0.303	35.09	0.042	264.41
$2.5t_0$	0.581	11.73	-0.221	31.21	0.030	336.81
$3.0t_0$	0.500	9.61	-0.120	31.34	0.021	424.09
$3.5t_0$	0.461	7.69	-0.057	34.54	0.014	530.22
$4.0t_0$	0.457	6.27	-0.026	40.54	0.009	660.50
$4.5t_0$	0.473	5.27	-0.012	48.97	0.006	820.34
$5.0t_0$	0.497	4.58	-0.006	57.87	0.004	1014.4
$5.5t_0$	0.522	4.12	-0.003	61.39	0.003	1244.2
$6.0t_0$	0.546	3.82	-0.003	52.30	0.003	1511.2

(b) $\eta/t_0 = 2.0$

	$P(t) - P_{\text{thermal}} = \sum_{i=1}^{2} a_i \exp(-t/\tau_i)$			
U	a_1	$\tau_1(t_0/\hbar)$	a_2	$\tau_2(t_0/\hbar)$
$0.0t_0$	0.846	0.63	-0.225	6.54
$0.5t_0$	0.830	0.67	-0.209	6.10
$1.0t_0$	0.818	0.72	-0.200	5.71
$1.5t_0$	0.810	0.78	-0.197	5.25
$2.0t_0$	0.804	0.85	-0.197	4.73
$2.5t_0$	0.805	0.95	-0.205	4.09
$3.0t_0$	0.882	1.14	-0.294	3.00
$3.5t_0$	0.852	1.03	-0.179	3.07
$4.0t_0$	0.776	0.90	-0.025	7.67
$4.5t_0$	0.591	1.25	-0.005	17.00
$5.0t_0$	0.551	1.50	0.009	7.74
$5.5t_0$	0.517	1.70	0.037	7.26
$6.0t_0$	0.482	1.89	0.069	7.30

[1] G. Stefanucci and R. van Leeuwen, *Nonequilibrium Many-Body Theory of Quantum Systems: A Modern Introduction* (Cambridge University Press, 2013).

[2] A. Nitzan, *Chemical Dynamics in Condensed Phases: Relaxation, Transfer and Reactions in Condensed Molecular Systems* (Oxford University Press, 2006).

[3] A. Szabo and N. S. Ostlund, *Modern Quantum Chemistry* (McGraw-Hill, New York, 1989).

[4] A. L. Fetter and J. D. Walecka, *Quantum Theory of Many-Particle Systems* (McGraw-Hill, Boston, 1971).

[5] H. Breuer and F. Petruccione, *Theory of Open Quantum Systems* (Clarendon, 2006).

[6] M. A. Schlosshauer, *Decoherence: and the Quantum-To-Classical Transition* (Springer, 2007).

[7] E. Joos, H. D. Zeh, C. Kiefer, D. J. W. Giulini, J. Kupsch, and I. O. Stamatescu, *Decoherence and the Appearance of a Classical World in Quantum Theory*, 2nd ed. (Springer, 2003).

[8] W. Kohn, Rev. Mod. Phys. **71**, 1253 (1999).

[9] J. A. Pople, Rev. Mod. Phys. **71**, 1267 (1999).

[10] H. Hwang and P. J. Rossky, J. Phys. Chem. B **108**, 6723 (2004).

[11] B. J. Schwartz, E. R. Bittner, O. V. Prezhdo, and P. J. Rossky, J. Chem. Phys. **104**, 5942 (1996).

[12] I. Franco and P. Brumer, J. Chem. Phys. **136**, 144501 (2012).

[13] G. S. Engel, T. R. Calhoun, E. L. Read, T.-K. Ahn, T. Mancal, Y.-C. Cheng, R. E. Blankenship, and G. R. Fleming, Nature **446**, 782 (2007).

[14] E. Collini, C. Y. Wong, K. E. Wilk, P. M. Curmi, P. Brumer, and G. D. Scholes, Nature **463**, 644 (2010).

[15] L. A. Pachón and P. Brumer, J. Phys. Chem. Lett. **2**, 2728 (2011).

[16] A. Chenu and G. D. Scholes, Annu. Rev. Phys. Chem. **66**, 69 (2015).

[17] R. Kapral, J. Phys.: Condens. Matter **27**, 073201 (2015).

[18] H. M. Jaeger, S. Fischer, and O. V. Prezhdo, J. Chem. Phys. **137**, 22A545 (2012).

[19] M. Shapiro and P. Brumer, *Quantum Control of Molecular Processes* (Wiley, 2012).

[20] M. A. Nielsen and I. L. Chuang, *Quantum Computation and Quantum Information* (Cambridge University Press, 2010).

[21] P. O. Löwdin, Adv. Chem. Phys. **2**, 207 (1959).

[22] P. Ziesche, Int. J. Quantum Chem. **56**, 363 (1995).

[23] R. Grobe, K. Rzazewski, and J. Eberly, J. Phys. B: At. Mol. Phys. **27**, L503 (1994).

[24] M. Nest, M. Ludwig, I. Ulusoy, T. Klamroth, and P. Saalfrank, J. Chem. Phys. **138**, 164108 (2013).

[25] W. Kutzelnigg and D. Mukherjee, J. Chem. Phys. **110**, 2800 (1999).

[26] I. Franco and H. Appel, J. Chem. Phys. **139**, 094109 (2013).

[27] A. D. Gottlieb and N. J. Mauser, Phys. Rev. Lett. **95**, 123003 (2005).

[28] A. D. Gottlieb and N. J. Mauser, Int. J. Quant. Inf. **5**, 815 (2007).

[29] J. Förstner, C. Weber, J. Danckwerts, and A. Knorr, Phys. Rev. Lett. **91**, 127401 (2003).

[30] A. Vagov, V. M. Axt, and T. Kuhn, Phys. Rev. B **66**, 165312 (2002).

[31] Y. Tanimura and R. Kubo, J. Phys. Soc. Jpn. **58**, 101 (1989).

[32] Q. Shi, L. Chen, G. Nan, R.-X. Xu, and Y. Yan, J. Chem. Phys. **130**, 084105 (2009).

[33] Y. Zhou and J. Shao, J. Chem. Phys. **128**, 034106 (2008).

[34] R.-X. Xu, P. Cui, X.-Q. Li, Y. Mo, and Y. Yan, J. Chem. Phys. **122**, 041103 (2005).

[35] P. Brumer and M. Shapiro, Proc. Natl. Acad. Sci. U. S. A. **109**, 19575 (2012).

[36] O. V. Prezhdo and P. J. Rossky, J. Chem. Phys. **107**, 5863 (1997).

[37] M. Bonitz, *Quantum Kinetic Theory* (Teubner, Stuttgart, 1998).

[38] R. K. Preston and J. C. Tully, J. Chem. Phys. **54**, 4297 (1971).